Sturmian function approach and $\overline{NN}$ bound states

Y. Yan and R. Tegen
Department of Physics, University of the Witwatersrand, WITS 2050, Johannesburg, South Africa

T. Gutsche and A. Faessler
Institut für Theoretische Physik, Universität Tübingen, Auf der Morgenstelle 14, D-72076 Tübingen, Germany
(Received 19 August 1996)

A suitable numerical approach based on Sturmian functions is employed to solve the $\overline{NN}$ bound state problem for local and nonlocal potentials. The approach accounts for both the strong short-range nuclear potential and the long-range Coulomb force and provides directly the wave function of protonium and $\overline{NN}$ deep bound states with complex eigenvalues $E=E_R-i(\Gamma/2)$. The spectrum of $\overline{NN}$ bound states has two parts, the atomic states bound by several keV, and the deep bound states which are bound by several hundred MeV. The observed very small hyperfine splitting of the $1s$ level and the $1s$ and $2p$ decay widths are reasonably well reproduced by both the Paris and Bonn potentials (supplemented with a microscopically derived quark annihilation potential), although there are differences in magnitude and level ordering. We present further arguments for the identification of the $^{13}PF_2$ deep bound state with the exotic tensor meson $f_2(1520)$. Both investigated models can accommodate the $f_2(1520)$ but differ greatly in the total number of levels and in their ordering. The model based on the Paris potential predicts the $^{13}P_0$ level slightly below 1.1 GeV while the model based on the Bonn potential puts this state below 0.8 GeV. It remains to be seen if this state can be identified with a scalar partner of the $f_2(1520)$. [S0556-2813(97)01408-8]

PACS number(s): 13.75.Cs, 02.60.−x, 14.40.Cs, 36.10.−k

I. INTRODUCTION

Replacing an electron orbiting around a nucleus in an atom with a heavier, negatively charged particle has opened up new windows in nuclear and particle physics. In the last three decades ''muonic'' [1] and ''pionic'' [2] atoms have been the focus of much theoretical and experimental efforts at various ''pion factories'' (LAMPF, PSI, TRIUMF). More recently the even heavier, negatively charged, antiproton $\overline{p}$ has become available in sufficient numbers to probe the nucleus at much smaller distances. Very low-energetic $\overline{p}$ can be ''trapped'' to form ''antiprotonic atoms.'' These allow us to study the interference of QED and QCD on the one hand, and the strong interaction (QCD) in the form of the annihilation into mesons, with unprecedented sensitivity, on the other hand. The simplest antiprotonic atom is the antiprotonic hydrogen atom known as ''protonium.'' The $\overline{p}p$ system can have quantum numbers unavailable to the e^+e^- system and, therefore, is particularly suited to study ''exotic'' (i.e., non-$\overline{Q}Q$) mesons. In this paper we wish to investigate the possibility that the firmly established broad tensor meson $f_2(1520)$ is a $\overline{NN}$ deep bound state.[1] The tensor meson $f_2(1520)$ is reported in protonium annihilations such as $\overline{NN}\rightarrow\pi f_2$ and $\overline{NN}\rightarrow\pi\pi f_2$ (see ASTERIX (1989) [3], Crystal Barrel (1991) [4]). Theoretical predictions for the production rate of the $f_2(1520)$ depend strongly on the wave functions of the initial and final states [5–8]. We employ here a powerful and well-documented mathematical method (not previously applied to $\overline{NN}$ bound states), known in atomic physics as the Sturmian function approach. With this method $\overline{NN}$ atomic states, arising from the interference of the long-ranged Coulomb interaction with the short-ranged strong interaction of QCD, can reliably be evaluated. Unlike the traditionally used Numerov method, the here employed Sturmian function approach can also be applied to nonlocal potentials (such as the Bonn potential) and to atomic states with higher angular momenta.

In recent years several experiments have been carried out at the low-energy antiproton ring LEAR at CERN to study the properties of protonium. In these experiments low energetic antiprotons are captured into the Coulomb field of the proton via Auger electron emission, after deceleration to a kinetic energy of a few eV [9]. In the case of hydrogen, $\overline{p}$ are captured into orbits of $n_{\overline{p}}\approx 40$ and cascade rapidly to the $1s$ and $2p$ levels (by x-ray emission), from which the $\overline{p}p$ system annihilates mostly into multimeson final states (occasionally those multimeson states are observed to be correlated via πf_2, $\pi\pi f_2$, etc.). The strong interaction shifts the Coulombic binding energies of the $1s$ and $2p$ states and adds a finite width describing the annihilation from this state. For a $\overline{p}p$ atom the purely Coulombic $1s$ Bohr radius is calculated to be 57.6 fm with a binding energy of $E_{1s}=12.49$ keV. The electromagnetic energies for the Lyman $K_\alpha(2p\rightarrow 1s)$, Balmer $L_\alpha(3d\rightarrow 2p)$, and Paschen $M_\alpha(4f\rightarrow 3d)$ transitions have been calculated; they are 9.367, 1.735, and 0.607 keV, respectively. The strong interaction splits the $1s$ state into $^1S_0$ and $^3S_1$, and the $2p$ state into $^3P_0$, $^3P_2$, $^1P_1$, and $^3P_1$. In principle, these energy levels can be determined by measuring the emitted x rays in the electromagnetic transitions. It is, however, extremely dif-

[1]The $f_2(1520)$ observed in $\overline{NN}$ annihilations was originally known as the AX tensor meson.

ficult to measure such small energy splittings (less than 0.5 keV). Therefore, the first experiments [10] delivered only spin-averaged data, since the experimental resolution was not sufficient to separate the transitions to the $^1S_0$ and $^3S_1$ levels. Recent measurements [11] at LEAR yielded the first information on the spin dependence of the $1s$ protonium energy shift and width.

Theoretical interest in the properties of protonium arose long before the first experiments were performed. Bryan and Phillips [12] first studied the scattering lengths of the $\overline{p}p$ annihilation at rest in their model of $\overline{NN}$ interaction. From the scattering lengths, the energy shifts and widths of $\overline{NN}$ atoms can be derived via Trueman's formula [13]. Later, the energy shift and width of protonium states were investigated by other groups using either the original Trueman's formula [14,15] or an improved Trueman's approach [16], or a WKB approximation [17] or an iteration technique which, however, neglected the $\overline{n}n$ component [18]. More accurate studies of the protonium properties were carried out in the matrix Numerov algorithm [19,20]. All these theoretical predictions for the energy shifts and widths of protonium states are consistent with available experimental data. In order to quantitatively evaluate the photon and pion emission in the reaction of protonium decay to $\overline{NN}$ deep bound states, Dover *et al.* [21] explicitly worked out the wave function of the $\overline{NN}$ $^1S_0$ and $^3S_1$ atomic states in the Numerov approach. In their calculation, the coupling of the $^3D_1$ and $^3S_1$ states is neglected. Using the numerical method developed in Ref. [20], they recalculate, in a later work [8], the wave functions of $\overline{NN}$ atomic states with the tensor coupling included. However, the wave function of $\overline{NN}$ atomic states for nonlocal $\overline{NN}$ potentials has not yet been evaluated in an accurate numerical method which takes into account the two length scales involved, the $\overline{p}p$ and $\overline{n}n$ component coupling and the tensor coupling of the nuclear force. In the present work, we solve the Schrödinger equation for $\overline{NN}$ bound states employing a properly adapted numerical method. The method accounts for both the strong *short*-range nuclear potential (local and nonlocal) and the *long*-range Coulomb force and provides directly the wave function of the protonium system and of the $\overline{NN}$ deep bound states with complex eigenvalues $E=E_R-i(\Gamma/2)$. Details of this method can be found below, in Sec. III.

The protonium states also provide a new tool for meson spectroscopy, which is still an active field exhibiting many open questions. The physics of mesons is far from complete although the quark model has been remarkably successful in understanding and classifying most of the experimentally well-established mesons as $Q\overline{Q}$ bound states. However, in recent years there has been a variety of experiments, for example πN scattering, $\overline{NN}$ annihilation, J/Ψ decay, and e^+e^- annihilation, which suggest the existence of new mesons which do not fit into the usual $Q\overline{Q}$ multiplets of flavor SU(N_f). These new meson states might be glueballs ggg, hybrids $Q\overline{Q}g$, or four quark-antiquark $Q^2\overline{Q^2}$ states as well as more ''conventional'' resonances such as $\overline{NN}$ bound states and meson-meson molecules. Recent reviews, concerning the status of non-$Q\overline{Q}$ states, are found in Ref. [22].

Exotic mesons come in two varieties: (i) meson resonances with quantum numbers $J^{PC}=0^{--}$, 0^{+-}, 1^{-+}, 2^{+-}, etc., which are unaccessible to $Q\overline{Q}$ pairs and (ii) meson resonances with anomalous decay modes and/or isolated production modes. The first evidence for a meson resonance under (i) with $J^{PC}=1^{-+}$ came from the GAMS Collaboration [23] which investigated the charge exchange reaction $\pi^- p\to nX_0$ ($X_0\to\pi^0\eta$). There is more evidence for meson resonances under (ii). Broad mesons X (with a width $\Gamma_X>50$ MeV) have been seen in the reactions $\overline{NN}\to\pi X$ and $\overline{NN}\to\pi\pi X$ from initial atomic states of orbital angular momentum $L=0,1$, as discussed above. Such mesons have typical hadronic sizes and lie in the mass range around 1.5 GeV. The best candidate, seen in different decay modes, has been the tensor meson $f_2(1520)$ with the quantum numbers $J^{PC}(I^G)=2^{++}(0^+)$. Note that $f_2(1520)$ appearing in the full listing of the Review of Particle Properties [41] was originally named $AX(1565)$ by the ASTERIX Collaboration [3]. The $f_2(1520)$ should not be confused with the meson $f_2'(1525)$ which has quite different decay modes. The $f_2'(1525)$ decays mostly into $\overline{K}K$ while the $f_2(1520)$ favors nonstrange mesons. In this paper, we concentrate on the identification of the exotic tensor meson $f_2(1520)$ as the $\overline{NN}$ deep bound state $^{13}PF_2$. It is interesting to note that an exotic tensor meson with the same quantum numbers and in the same mass range features prominently in the reactions $\overline{p}p\to\pi\pi$, $\overline{K}K$ [24].

The $N\overline{N}$ deep bound state spectrum has been calculated in a variety of local potential models. So far no calculation has been reported for nonlocal potentials. In one-boson exchange potential (OBEP) models, the elastic part of the $N\overline{N}$ interaction is described in terms of meson exchange which may be obtained from a G-parity transform of a suitable nucleon-nucleon (NN) model. The real, elastic part must be supplemented with an absorptive potential, reflecting the short-ranged annihilation into mesonic final states. Model predictions for $N\overline{N}$ bound states usually apply an annihilation part which is either described by a phenomenological optical potential [25–27], adjusted to fit low-energy $N\overline{N}$ scattering data, or derived microscopically in so-called rearrangement versions of the quark model [28,29]. The original theoretical expectation for the existence of $N\overline{N}$ deep bound states was very much in line with the first tentative experimental evidence for narrow (decay widths $\Gamma\leqslant 20$ MeV) resonances coupled to the $N\overline{N}$ system. However, high-precision experiments at the Low Energy Antiproton Ring (LEAR) at CERN subsequently dismissed this early evidence for the production of narrow ($\Gamma\leqslant 20$ MeV) states in $N\overline{N}$ annihilation [30].

In the next section we give details of our treatment of $\overline{NN}$ atomic states and in Sec. III we present the Sturmian function approach to solve the coupled equations for $\overline{NN}$ atoms accounting for the $\overline{NN}$ tensor force and the $\overline{n}n$ component in local and nonlocal $\overline{NN}$ models. This is the central part of our paper. Section IV follows with our results for $\overline{NN}$ bound states in a microscopically derived potential model, and a

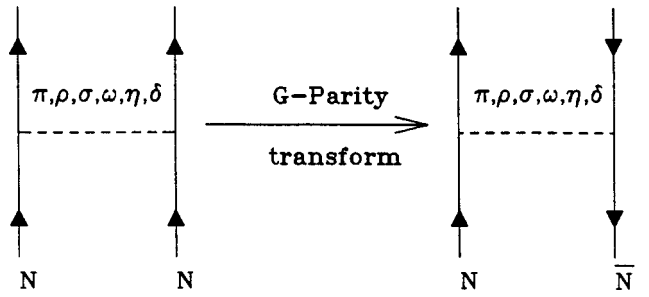

FIG. 1. G-parity transformation of a one boson-exchange NN potential to its $\overline{NN}$ version.

comparison with experiments and other models. The section ends with our conclusions.

II. THE SCHRÖDINGER EQUATION FOR $\overline{NN}$ ATOMIC STATES

A correct treatment of $\overline{NN}$ atomic states must include the coupling of the proton-antiproton ($\overline{pp}$) and neutron-antineutron ($\overline{nn}$) configurations. We define the Hilbert spaces of proton-antiproton and neutron-antineutron by P_1 and P_2 projection operators, respectively. The Hilbert space of meson channels is defined as Q space. The corresponding projection operators P_1, P_2, and Q satisfy the completeness relation

$$P_1+P_2+Q=1, \tag{1}$$

as well as orthogonality

$$P_1P_2=P_2P_1=0, \tag{2}$$

$$P_1Q=QP_1=0, \tag{3}$$

$$P_2Q=QP_2=0. \tag{4}$$

Let H be the Hamilton operator of the full coupled-channel with the corresponding wave function $|\psi\rangle$ defined in the complete Hilbert space. We eliminate meson final state interactions, resulting in the coupled set of equations for the $\overline{pp}$ and $\overline{nn}$ wave function:

$$(E-P_1HP_1)P_1|\psi\rangle=P_1HQGQHP_1P_1|\psi\rangle+P_1HP_2P_2|\psi\rangle + P_1HQGQHP_2P_2|\psi\rangle, \tag{5}$$

$$(E-P_2HP_2)P_2|\psi\rangle=P_2HQGQHP_2P_2|\psi\rangle+P_2HP_1P_1|\psi\rangle + P_2HQGQHP_1P_1|\psi\rangle, \tag{6}$$

where E is the energy eigenvalue and G is the Greens function for meson intermediate states, defined as

$$G=\frac{1}{E-QHQ}. \tag{7}$$

The interaction terms in Eqs. (5) and (6) are given as

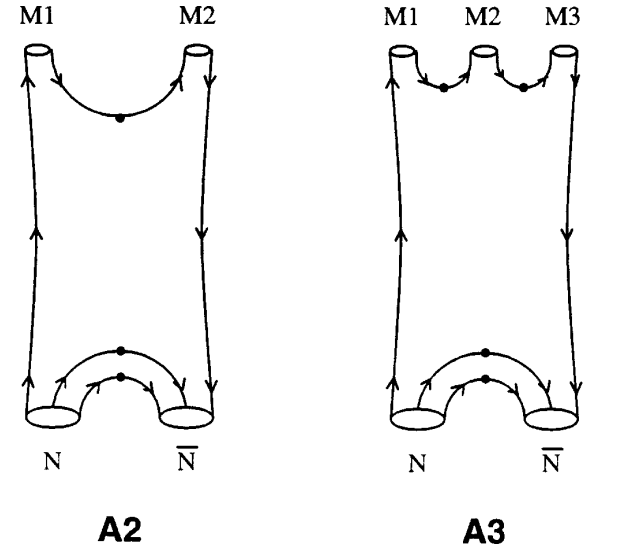

FIG. 2. $\overline{NN}$ annihilation into two and three mesons in the nonrelativistic $^3P_0$ quark model.

$$P_1HP_1=H_0^p+V_c+V_{\rm EL}, \tag{8}$$

$$P_2HP_2=H_0^n+V_{\rm EL}, \tag{9}$$

$$P_1HP_2=P_2HP_1=V_{\rm CEX}, \tag{10}$$

where V_c is the Coulomb interaction. $H_0^p=\sqrt{m_p^2+\vec{k}^2}$ and $H_0^n=\sqrt{m_n^2+\vec{k}^2}$ are the free energies of the proton and neutron, respectively. The masses of the proton and neutron are denoted as m_p and m_n. The elastic potential $V_{\rm EL}$ and the charge-exchange potential $V_{\rm CEX}$ are combinations of the isopin $I=0$ and $I=1$ meson-exchange potentials corresponding to the process in Fig. 1, such as $V_{\rm EL}=\frac{1}{2}(V^0+V^1)$ and $V_{\rm CEX}=\frac{1}{2}(V^0-V^1)$.

$P_iHQGQHP_j$ are the optical potentials, denoted by W for $\overline{NN}$ annihilation into two and three mesons in Fig. 2:

$$W_{\rm EL}=P_1HQGQHP_1=P_2HQGQHP_2=\frac{1}{2}(W^0+W^1), \tag{11}$$

$$W_{\rm CEX}=P_1HQGQHP_2=P_2HQGQHP_1=\frac{1}{2}(W^0-W^1), \tag{12}$$

where $W^{0,1}$ are the annihilation potentials for isospin $I=0$, 1 $\overline{NN}$ states.

As an example, we give the final equation for spin-triplet $\overline{NN}$ states in the $\{J,L,S\}$ basis as

$$\begin{pmatrix} H_{11} & H_{12} \\ H_{21} & H_{22} \end{pmatrix}\begin{pmatrix} \Psi_{\overline{pp}} \\ \Psi_{\overline{nn}} \end{pmatrix}=-E_b\begin{pmatrix} \Psi_{\overline{pp}} \\ \Psi_{\overline{nn}} \end{pmatrix}, \tag{13}$$

with

$$H_{11}=\begin{pmatrix} P^2/2\mu+V_c^{L_1L_1}+V_{\rm EL}^{L_1L_1}+W_{\rm EL}^{L_1L_1} & V_{\rm EL}^{L_1L_2} \\ V_{\rm EL}^{L_2L_1} & P^2/2\mu+V_c^{L_2,L_2}+V_{\rm EL}^{L_2,L_2}+W_{\rm EL}^{L_2,L_2} \end{pmatrix}, \tag{14}$$

$$H_{12}=\begin{pmatrix} V_{\rm CEX}^{L_1L_1}+W_{\rm CEX}^{L_1L_1} & V_{\rm CEX}^{L_1L_2} \\ V_{\rm CEX}^{L_2L_1} & V_{\rm CEX}^{L_2,L_2}+W_{\rm CEX}^{L_2,L_2} \end{pmatrix}=H_{21}^T, \tag{15}$$

$$H_{22}=\begin{pmatrix} P^2/2\mu+2\,\delta m+V_{\rm EL}^{L_1L_1}+W_{\rm EL}^{L_1L_1} & V_{\rm EL}^{L_1L_2} \\ V_{\rm EL}^{L_2L_1} & P^2/2\mu+2\,\delta m+V_{\rm EL}^{L_2,L_2}+W_{\rm EL}^{L_2,L_2} \end{pmatrix}, \tag{16}$$

and

$$\Psi_{\overline{pp}}=\begin{pmatrix} \Psi_{\overline{pp}}^{L_1} \\ \Psi_{\overline{pp}}^{L_2} \end{pmatrix}, \quad \Psi_{\overline{nn}}=\begin{pmatrix} \Psi_{\overline{nn}}^{L_1} \\ \Psi_{\overline{nn}}^{L_2} \end{pmatrix}, \tag{17}$$

where $\delta m=m_n-m_p$, $\mu=m_p/2$, $V_c=-\alpha/r$, $L_1=J-1$, $L_2=J+1$, J is the total angular momentum, and $E_b=2m_p-E$ the binding energy of $\overline{NN}$ atomic states. Note that the final equation for protonium is in a nonrelativistic form. Our calculation shows that the predictions obtained with the relativistic and nonrelativistic equations are not noticeably different.

III. COMPLETE SET OF STURMIAN FUNCTIONS

In principle, one could solve Eq. (13) through expanding the $\overline{NN}$ wave functions $\Psi_{\overline{pp}}$ and $\Psi_{\overline{nn}}$ in any complete set of orthonormal functions. The complete set of harmonic oscillator wave functions is widely applied to bound state problems since they have analytical forms both in coordinate and momentum spaces. Bound state problems with only the strong interaction or only the Coulomb force can be well solved in the regime of harmonic oscillator wave functions, by choosing the oscillator length being of order 1 or 100 fm, respectively. Detailed investigations [31], however, have shown that the harmonic oscillator wave function approach fails to describe $\overline{NN}$ atomic states which are dominated by the long-ranged Coulomb force and influenced by the short-ranged strong interaction. The reason is that two very different oscillator lengths are involved to describe the $\overline{NN}$ deep bound state *and* the atomic state.

The Sturmian function method was first used in atomic physics to evaluate the binding energy and wave function of atoms [32,33]. It was pointed out that the method is much more powerful than the approach using harmonic oscillator and hydrogen wave functions. Subsequently, the method was applied to various physical problems such as electromagnetic collisions [34], binding energies of nuclei [35,36], and bound and resonant states in special potentials [37,38]. The Sturmian functions are very similar to the hydrogen wave functions and are, therefore, also named Coulomb-Sturmian functions. In coordinate space the Sturmians $S_{nl}(r)$, which are used in the present work, satisfy the second-order differential equation [34]

$$\left(\frac{d^2}{dr^2}-\frac{l(l+1)}{r^2}+\frac{2b(n+l+1)}{r}-b^2\right)S_{nl}(r)=0. \tag{18}$$

By solving Eq. (18), one finds

$$S_{nl}(r)=\left[\frac{n!}{(n+2l+1)!}\right]^{1/2}(2br)^{l+1}\exp(-br)L_n^{2l+1}(2br), \tag{19}$$

where $L_n^{2l+1}(x)$ are Laguerre polynomials. The Sturmians are orthogonal and form a complete set with respect to the weight function $1/r$, which follows from the corresponding $1/r$ potential term in Eq. (18):

$$\int_0^\infty r^2dr\,\frac{S_{nl}(r)}{r}\,\frac{1}{r}\,\frac{S_{n'l}(r)}{r}=\delta_{nn'}. \tag{20}$$

Thus radial functions $R_l(r)$ can be expanded in the complete set of the Sturmian functions $S_{nl}(r)$,

$$R_l(r)=\sum_n\, a_{nl}\frac{S_{nl}(r)}{r}. \tag{21}$$

Inserting Eq. (21) into Eq. (13) does not lead to a diagonal form on the right-hand side of Eq. (13) unlike the case of the harmonic oscillator wave functions. The matrices on both sides of Eq. (13) must be simultaneously diagonalized. Note that the Sturmians have analytical form [34] in momentum space. One is allowed to deal with strong interactions in momentum space with the complete set of the Sturmians as easily as with the set of the harmonic oscillator wave functions. The matrix elements of the Coulomb interaction as well as the kinetic term can be evaluated analytically according to Eq. (18) and Eq. (20).

Because almost all bound-state hydrogenic wave functions are close to zero energy, the innermost zeros of the functions are insensitive to the principle quantum number. This accounts for the fact that the bound hydrogen functions do not form a complete set; the continuum is needed to ana-

lyze the region between the origin and the limiting first zero. Unlike hydrogen functions, the first node of the Sturmian functions continues to move closer to the origin with increasing the principle number n. This is the key point why a short-ranged nuclear force can easily be taken into account for the $\overline{NN}$ atomic state problem by using complete sets of the Sturmian functions.

The parameter b is the length scale entering the Sturmian functions in Eqs. (18) and (19), in the same way as the corresponding parameter enters the harmonic oscillator functions. For $\overline{NN}$ deep bound states one should use $1/b$ of order 1 fm while the atomic states without strong interactions require $1/b$ of order 10^2 fm. However, for protonium accounting for both the strong interaction and the Coulomb force, one must use a $1/b$ between the two values used for the above cases. Using a complete basis of, for example, 200 Sturmian functions (100 for the $L=J-1$ wave, and another 100 for the $L=J+1$ wave) with $1/b=5-500$ fm, one can precisely reproduce the analytical $1s$ and $2p$ wave functions of the $\overline{NN}$ system subject to only the Coulomb interaction. Using the same basis with $1/b=0.1-30$ fm, the wave functions of $\overline{NN}$ deep bound states can be precisely evaluated. The $\overline{NN}$ deep bound states can be evaluated in the complete set of the harmonic oscillator wave functions, and also in the complete set of Sturmian functions with a more suitable length parameter, for example, $1/b=1$ fm. From the above investigation, a length parameter $1/b$ around 20 fm is suitable for the protonium problem.

We have compared our numerical method with the traditionally used method, namely, the Numerov approach [20], applied to the $\overline{NN}$ atomic problem in, for example, the Kohno-Weise potential. The binding energies and widths presented in Ref. [20] for the states $^1S_0$, $^3P_0$, $^3S_1$, and $^3SD_1$ are well reproduced in the Sturmian function approach. Wave functions for these states are also compared in the two approaches. Here only the wave functions for the state $^3SD_1$ are presented in Fig. 3. It is found that at short distance the outputs in the two approaches are quite consistent, and that the discrepancies between the wave functions evaluated in the two methods become more and more obvious as the relative distance between nucleon and antinucleon increases, especially the imaginary part of the $^1S_0$ and $^3S_1$ wave functions.

Finally, it should be pointed out that the Numerov method cannot be applied to a nonlocal potential, for example, the Bonn potential which is given in momentum space, and it is not easy to handle atomic states with higher angular momentum [39], for example, the state $^3PF_2$. Therefore it is essential to use a precise numerical method, applied not only to local but also to nonlocal potentials, to handle the $\overline{NN}$ atomic state problem from a more general point of view. In principle, there is no limit to the accuracy in the evaluation of the $\overline{NN}$ atomic states in the Sturmian function approach. One is allowed to use larger and larger complete bases of the Sturmian functions until the theoretical results converge.[2] And

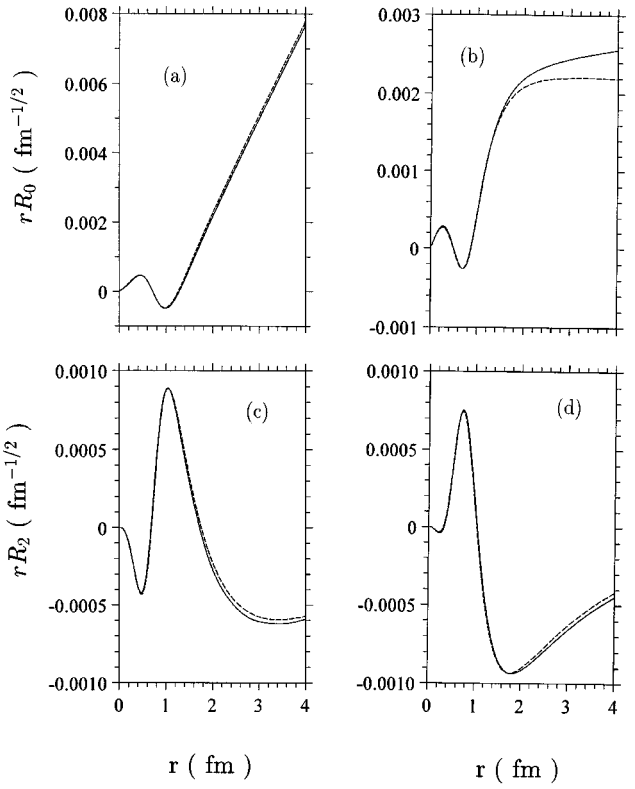

FIG. 3. The wave functions $rR_l(r)$ of the $\overline{NN}$ atomic states $^3SD_1$. Here only the $I=0$ part is presented. The solid curves are for the wave functions evaluated by Carbonell in the Numerov method [39], and the dashed curves represent our results. (a) the real part of the $^{13}S_1$ wave function, (b) the imaginary part of the $^{13}S_1$, (c) the real part of the $^{13}D_1$ wave function, and (d) the imaginary part of the $^{13}D_1$. The states are labeled according to $^{2I+1,2S+1}L_J$. And $\Psi^I=1/\sqrt{2}[\Psi^{\overline{pp}}+(-)^I\Psi^{\overline{nn}}]$.

the $\overline{NN}$ atomic states with higher angular momenta can be easily handled in the approach.

IV. $\overline{NN}$ BOUND STATES

A. Experiments on $\overline{NN}$ bound states

The properties of $\overline{NN}$ atomic states have been studied in several experiments [10,11] at LEAR. The results for energy shift ΔE and width Γ of the $1s$ and $2p$ atomic states are collected in Table I, where the energy shift ΔE is measured with respect to the pure Coulomb binding energy $E^0_{1s}=12.49$ keV, see Fig. 4(a). Except for the energy shift and width of the state $^3SD_1$ reported in Ref. [11], other data are available only at the spin-averaged level. All the experiments determined $\Delta E_{1s}<0$, which corresponds to a $1s$ state which is less bound, hence the effect of the strong interaction is repulsive. Theoretical predictions [12–20] for the energy shift ΔE_{1s} and widths Γ_{1s} and Γ_{2p} are in reasonable agreement with the experimental data except for the quark rearrangement model [40]. In addition to the measurement of the properties of $\overline{pp}$ atoms, another important result of recent LEAR experiments is the evidence for broad mesonic resonances (decay widths $\Gamma\geqslant 50$ MeV) which cannot be fitted into the usual $Q\overline{Q}$ flavor multiplets. One prominent example

[2]There is no CPU problem, most university computers are capable enough.

TABLE I. Experimental energy shifts ΔE and widths Γ for $N\overline{N}$ atomic states.

ΔE_{1s} (keV)	Γ_{1s} (keV)	Γ_{2p} (meV)	Refs.
-0.50 ± 0.30	< 1.0		Ahmad *et al.* (1985) [10]
-0.70 ± 0.15	1.60 ± 0.40		Ziegler *et al.* (1988) [10]
-0.75 ± 0.06	0.90 ± 0.18	45 ± 10	Baker *et al.* (1988) [10]
-0.73 ± 0.05	1.13 ± 0.09		Van Eijk *et al.* (1988) [10]
-0.62 ± 0.10	1.13 ± 0.17	32 ± 10	Bacher *et al.* (1989) [10]
-0.73 ± 0.02	1.12 ± 0.06	34 ± 2.9	K. Heitliner *et al.* (1993) [11]
-0.85 ± 0.04 ($^3SD_1$)	0.77 ± 0.15 ($^3SD_1$)		

is the tensor meson $f_2(1520)$ [41] with quantum numbers $J^{PC}(I^G)=2^{++}(0^+)$ and mass near 1530 MeV, for which there was some evidence in earlier bubble chamber experiments [42]. The ASTERIX group at LEAR studied the reaction $p\overline{p}\to\pi^+\pi^-\pi^0$ from a pure initial $L=1$ atomic state and established the tensor meson $AX(1565)$, which appears

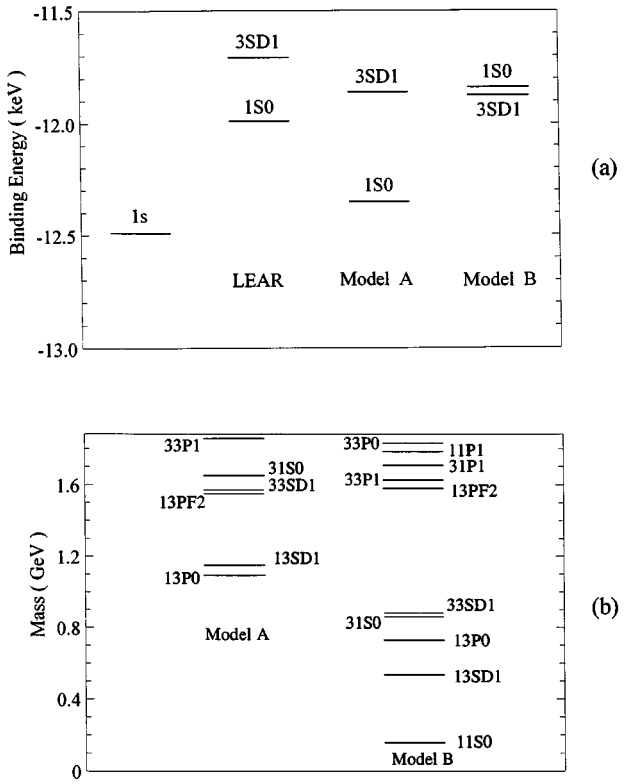

FIG. 4. (a) $\overline{NN}$ atomic states given in the binding energy $-E_{1s}=-2m_p+E$. The left state is the unperturbed Coulombic $1s$ state. The column labeled ''LEAR'' represents the Monte Carlo simulation result [55], the columns labeled ''model A'' and ''model B'' refer to the Paris and Bonn potentials, respectively. (b) $\overline{NN}$ deep bound states given in total energies (masses). Note that $f_2(1520)$ has the same quantum numbers as the $^{13}PF_2$ state, f_0 has the same quantum numbers as the $^{13}P_0$ state. Similarly other mesons could be associated with energy levels of the spectrum. Only $f_2(1520)$ is a firm candidate, other identifications are speculative. Model A puts such an f_0 at $\sim$1100 MeV while model B puts it below 800 MeV. The notation for the states is $(2I+1)(2S+1)LJ$. That two different values L and $L+2$ as in SD, PF, etc., are given indicates their mixing in this state.

in the full listing of the Review of Particle Properties [41] as $f_2(1520)$, in the $\pi^+\pi^-$ channel [3]. First results obtained by the Crystal Barrel Collaboration for $p\overline{p}\to 3\pi^0$ in liquid hydrogen (which is dominated by initial $L=0$ atomic states, and associated with initial $L=1$ atomic states) also revealed the presence of the $f_2(1520)$ resonance in the $\pi^0\pi^0$ D-wave annihilation channel [4]. However, a later analysis of the Crystal Barrel data for $p\overline{p}\to 3\pi^0$ together with $p\overline{p}\to\eta\eta\pi^0$ [43], imposing $p\overline{p}$ S states only, also indicated the presence of an isoscalar-scalar $J^{PC}=0^{++}$ resonance with a mass of 1520 MeV, where the contribution of the $f_2(1520)$ is reduced [44]. The latest partial-wave analysis of the reaction $p\overline{p}\to 3\pi^0$ in liquid hydrogen, relaxing the previous constraint of pure $p\overline{p}$ S-state annihilation, indicates both the need for a scalar 0^{++} and a tensor 2^{++} state in the $\pi^0\pi^0$ annihilation channels [45]. The respective values for mass M and width Γ of these two resonances are [45]

$$f_0(1500): M=1500\ \text{MeV},\quad \Gamma=120\ \text{MeV},$$
$$J^{PC}(I^G)=0^{++}(0^+), \tag{22}$$

and

$$f_2(1520)/AX: M=1530\ \text{MeV},\quad \Gamma=135\ \text{MeV},$$
$$J^{PC}(I^G)=2^{++}(0^+). \tag{23}$$

The analysis [27], which demonstrated that quantum numbers, production branching ratios, and relative strength of strong decay modes, are consistent with the interpretation of the $f_2(1520)$ as a tensor coupled $^{2I+1,2S+1}L_J=^{13}PF_2$ $N\overline{N}$ bound state. However, other interpretations, such as $\omega\omega/\rho\rho$ molecules [46], might also be tenable.

Although observed in the $\pi^+\pi^-$ and $\pi^0\pi^0$ channels, respectively, of the reactions $p\overline{p}\to\pi^+\pi^-\pi^0$ and $p\overline{p}\to\pi^0\pi^0\pi^0$, $f_2(1520)$ cannot have $\pi\pi$ as the dominant decay mode, since this $2^{++}(0^+)$ state has not been seen in $\pi\pi$ phase shift analyses and in the $\gamma\gamma\to\pi\pi$ process. The decays $f_2(1520)\to\eta\eta,\eta\eta'$ are shown to be small by Crystal Barrel and E760, and the $\omega\omega$ mode must be small because of phase space restrictions. Therefore, $f_2(1520)\to\rho\rho$ is likely to be the largest decay mode. This mode would be exceedingly difficult to detect as it requires ρ-like correlations among pion pairs in the final states including more than 4π. The nonrelativistic quark model $A2$ [47,48] in Fig. 2

TABLE II. The parameters adjusted to low-energy $\overline{NN}$ data.

Model A			Model B		
r_0 (fm)	λ_{A_2} (GeV^{-1})	λ_{A3} (GeV$^{-3/2}$)	Λ (GeV)	λ_{A_2} (GeV^{-1})	λ_{A3} (GeV$^{-3/2}$)
0.57−0.65	5.5−7.5	4.0−6.5	0.7−1.0	2.5−4.0	4.0−6.0

predicts indeed the dominance of the $\rho\rho$ decay mode of the $f_2(1520)$. Recently, evidence for a possible 2^{++} state at 1640 MeV decaying into $\rho^0\rho^0$ has been reported in the reaction $\overline{n}p \to \pi^+\pi^+\pi^+\pi^-\pi^-$ at high $\overline{n}$ momenta [49]. A 2^{++} resonance with mass $\sim$ 1640 MeV and $\Gamma \leqslant 70$ MeV has also been seen in the final state $\omega\omega$ by the GAMS and VES Collaborations [50,51]. One might suppose that the $f_2(1520)$ and the 2^{++} resonance with mass 1640 MeV can be reduced to the same object.

B. Predictions for $\overline{NN}$ bound states

In this section, we use the Sturmian function approach to evaluate the mass and width of both the $\overline{NN}$ deep bound states and atomic states, with special emphasis on how the $\overline{NN}$ strong interaction influences the energy shift and width of $\overline{NN}$ atoms. We resort to a $N\overline{N}$ potential, where the absorption is derived in the nonperturbative quark annihilation model [47], the elastic part taken as the G-parity transformation of different meson-exchange models of the NN interaction, namely, as defined by versions of the Bonn [52] and Paris [53] groups.

The complex $N\overline{N}$ potential $V_{N\overline{N}}$ consists of an elastic and an annihilation part:

$$V_{N\overline{N}} = V_{\rm OBE} + V_{\rm ANN} + iW_{\rm ANN}. \tag{24}$$

The short-ranged imaginary part $W_{\rm ANN}$ describes annihilation into two and three meson final states, thereby also generating a dispersive real part $V_{\rm ANN}$. The microscopic derivation of the complex annihilation part $V_{\rm ANN} + iW_{\rm ANN}$ is done in a nonrelativistic quark model using the planar annihilation topology $A2$ and $A3$ [47] in Fig. 2. The effective $Q\overline{Q}$ annihilation/creation operator is described by the $^3P_0$ vertex, i.e., $Q\overline{Q}$ pairs are created/destroyed with vacuum quantum numbers: $J^{PC}(I^G) = 0^{++}(0^+)$ and $^3P_0$ in LS coupling. It is interesting to note that the relativistic annihilation model of [57] also finds a preference for the $^3P_0$ vertex. The overall strength of the respective two- and three-meson transitions are free phenomenological parameters given ultimately by nonperturbative QCD dynamics (gluonium spectrum, energy dependence of the strong coupling, etc.). The basis for the use of the planar quark models $A2$ and $A3$ is founded in the analysis of two meson production data for $N\overline{N}$ annihilation [48]. The derivation of the optical potential due to these annihilation diagrams is extensively discussed in Ref. [47]. The explicit consideration of the mesonic annihilation channels results in an energy- and state-dependent absorption potential, which is nonlocal.

The elastic part $V_{\rm OBE}$ is constructed by the G-parity transformation of a realistic one-boson exchange potential of the NN interaction, as illustrated in Fig. 1. In model A, we consider the G-parity transformed meson-exchange part of the NN Paris potential [53], containing π, 2π, and ω exchange. The short-range part of the elastic interaction has to be regularized by use of a cutoff, as introduced by the Helsinki group [28]:

$$f(r) = \frac{(r/r_0)^{10}}{1+(r/r_0)^{10}}. \tag{25}$$

In model B, we use the energy-independent one-boson exchange potential (OBEPQ) of the Bonn group [52]. A short-range regularization to the potential is applied [47], by applying the following cutoff function to the Bonn potential:

$$F(q,q',\Lambda) = \frac{1}{1+(q/\Lambda)^{10}} \cdot \frac{1}{1+(q'/\Lambda)^{10}}. \tag{26}$$

In the present work there are three parameters, namely (r_0, λ_{A_2}, λ_{A_3}) in model A and (Λ, λ_{A_2}, λ_{A_3}) in model B. These parameters are determined in three steps: first fitted to the experimental data of the charge-exchange, elastic, and inelastic integrated cross sections of the $\overline{p}p$ reaction [54], then to the $\overline{NN}$ atomic data, and finally to the exotic tensor meson $f_2(1520)$. The theoretical results for the integrated cross sections of the $\overline{p}p$ reaction are not sensitive to the parameters. Each parameter is adjusted into a range, but not a certain value [54]. Then we fit the preadjusted parameters to experimental data of $\overline{NN}$ atomic states. After these two steps, the parameters are bound into narrow ranges as listed in Table II. The freedoms of the parameters make the theoretical predictions for the energy levels and widths of the $\overline{NN}$ deep bound states uncertain. The binding energies of $\overline{NN}$ deep bound states depend strongly on the cutoffs r_0 and Λ. The uncertainties of the r_0 and Λ result in $\sim \pm 150$ MeV and $\sim \pm 200$ MeV to the $^{13}PF_2$ mass in models A and B, respectively. Compared to the cutoffs, the freedoms of λ_{A2} and λ_{A3} only affect the final result a little. The theoretical results for the energy shifts and widths of the atomic states $^1S_0$, $^3SD_1$, and $^3P_0$ are presented in Table III and Fig. 4(a) with a parameter such as $r_0 = 0.60$ fm, $\lambda_{A2} = 6.5$ GeV^{-1}, and $\lambda_{A3} = 5.5$ GeV$^{-3/2}$ in model A and $\Lambda = 0.8$ GeV, $\lambda_{A2} = 3.0$ GeV^{-1}, and $\lambda_{A3} = 5.0$ GeV$^{-3/2}$ in Model B. For comparison, the energy shifts and widths in the Monte Carlo simulation [55] of a planned LEAR experiment are also listed in the table. With the same parameters, we obtain the mass and width of the $\overline{NN}$ deep bound state $^{13}PF_2$ as

$$M_A = 1570 \text{ MeV}, \quad \Gamma_A = 110 \text{ MeV} \tag{27}$$

and

$$M_B = 1580 \text{ MeV}, \quad \Gamma_B = 90 \text{ MeV}, \tag{28}$$

TABLE III. The energy shifts and widths of the $1s$ and $2p$ $\overline{NN}$ atomic states, see also Fig. 4(a).

	Monte Carlo		Model A		Model B	
	ΔE (eV)	Γ (eV)	ΔE (eV)	Γ (eV)	ΔE (eV)	Γ (eV)
$^1S_0$	-500 ± 20	990 ± 73	-140	1020	-650	820
$^3SD_1$	-784 ± 4	660 ± 15	-630	725	-615	510
$^3P_0$	-0.100 ± 0.008	0.075 ± 0.015	-0.045	0.080	-0.050	0.060

for models A and B, respectively. The spectrum of $\overline{NN}$ deep bound states is presented in Fig. 4(b). The ratio of λ_{A3} to λ_{A2} found here is comparable with the value in Ref. [47]. Such values for r_0 and Λ are close to the annihilation radius as deduced from the convolution of the baryon number distribution in the $N\overline{N}$ system [56] as well as those derived from the effective quark-antiquark annihilation density [57].

The annihilation potential derived from the $A2$ and $A3$ $\overline{NN}$ annihilation diagrams supports reasonable widths for the $1s$ and $2p$ $\overline{NN}$ atomic states, see Table III. The prediction for the width of $1s$ $\overline{NN}$ atoms in a quark rearrangement model [40] is too small, compared to experimental data. This shows again that experiments prefer the $A2$ and $A3$ $\overline{NN}$ annihilation processes over the quark rearrangement model.

We find that it is extremely difficult to reproduce the Monte Carlo simulation results [55] and the experimental data [11], namely, both the energy shifts and widths with model A. If one employs a large enough annihilation potential derived from the $A2$ and $A3$ diagrams to fit the energy shift of the atomic state $^1S_0$, one obtains too large a width for the state.

We notice, in Fig. 4(b), that the predictions for the $\overline{NN}$ deep bound states are rather different in models A and B. While model A predicts no bound states below 1.0 GeV, model B has a proliferation of states in that region. The spectrum of model A looks to us more realistic than the one of model B. We recall that the λ_{A2}, λ_{A3}, and the cutoff Λ are adjusted to reproduce the properties of the $\overline{NN}$ $1s$ and $2p$ atomic states and to identify the $\overline{NN}$ deep bound state $^{13}PF_2$ with the exotic meson $f_2(1520)$. Note that the $f_2(1520)$ meson should not be confused with the tensor meson $f_2'(1525)$ [41]. The discrepancy between the spectra of models A and B indicates to us the need for a proper energy-dependent $\overline{NN}$ potential in momentum space which provides for the proper reduction in strength as the $\overline{NN}$ energy decreases below threshold. It should be pointed out that the energy-dependent Bonn potentials are not suitable for this.

The properties of $\overline{NN}$ atomic states are naturally sensitive to the $\overline{NN}$ strong interaction at threshold. The shift of protonium energy levels is dominated by both the long-distance π-exchange potential and the admixture of the $\overline{nn}$ component to $\overline{pp}$ atoms. The long-distance π-exchange $\overline{NN}$ interaction is model independent. One is forced to conclude that the difference between the $I=0$ and $I=1$ parts of the $\overline{NN}$ interaction for the $^1S_0$ state at threshold as derived from the NN Paris potential through a G-parity transformation, is apparently too small. The Bonn potential roughly reproduces the observed small energy shifts of the $1s$ atomic state but gives the wrong level ordering for the states $^1S_0$ and $^3SD_1$, see Fig. 4(a). For the $\overline{NN}$ deep bound state spectrum the situation is reversed; here the Paris potential looks more realistic than the Bonn potential. None of the investigated models is able to reproduce both the atomic and deep bound spectrum equally well.

In conclusion, the $\overline{NN}$ bound state spectrum represents a sensitive test for current NN and $\overline{NN}$ models. For the first time the $\overline{NN}$ spectrum has been calculated for a nonlocal potential in momentum space (the Bonn potential). The spectrum has two distinct parts, which are separated by a wide energy gap. The ''upper'' part consists of the atomic states which are several keV below the $\overline{NN}$ threshold of $2m_p=1.88$ GeV and which represent a large ($\sim10^2$ fm) system dominated by QED forces. The ''lower'' part of the spectrum consists of a presently unknown number of deep bound states, which are several hundred MeV below the $\overline{NN}$ threshold and have a much smaller, hadronic size (~1 fm) dominated by QCD forces. Only one state $^{13}PF_2$ has been identified with the exotic meson $f_2(1520)$ so far. On the theoretical side, the $\overline{NN}$ spectrum with its two very different parts and nonlocal $\overline{NN}$ potentials involved requires a new numerical approach. We have used here the Sturmian function approach which is shown to be particularly suited to the $\overline{NN}$ spectrum and wave functions. We find that the two models investigated (versions of the local Paris and nonlocal Bonn potentials supplemented with an optical potential derived in the $^3P_0$ quark model) either work well in the lower or in the upper part of the spectrum, but not in both parts. It is noteworthy that all Bonn potentials give a very deep bound state $^{11}S_0$ which is not so for the Paris potential. This can be traced back to differences in the isospin dependence of the two models. We also find a sensitivity of the spectrum to the *type* of the quark annihilation potential used ($^3P_0$ or others). Both models can accommodate $f_2(1520)$ as a $\overline{NN}$ deep bound state $^{13}PF_2$, but they differ significantly in the number and level ordering of other deep bound states. It will be interesting to see if other exotic mesons [for example the scalar partner of $f_2(1520)$] can be identified with members of the $\overline{NN}$ bound state spectrum.

ACKNOWLEDGMENT

We are grateful to J. Carbonell for communicating to us his numerical results for various protonium wave functions.

[1] V. W. Hugher, Annu. Rev. Nucl. Sci. **16**, 445 (1966); C. S. Wu and L. Wilets, *ibid.* **19**, 527 (1969).
[2] G. Backenstoss, Annu. Rev. Nucl. Sci. **20**, 467 (1970); E. H. S. Burhop, High Energy Phys. **3**, 109 (1969).
[3] B. May *et al.*, Phys. Lett. B **225**, 450 (1989); Z. Phys. C **46**, 191 (1990); **46**, 203 (1990).
[4] E. Aker *et al.*, Phys. Lett. B **260**, 249 (1991).
[5] J. A. Niskanen, V. Kuikka, and A. M. Green, Nucl. Phys. **A443**, 691 (1985).
[6] M. Kohno and W. Weise, Nucl. Phys. **A454**, 429 (1986).
[7] L. Mandrup *et al.*, Nucl. Phys. **A512**, 591 (1990).
[8] C. D. Dover, J.-M. Richard, and J. Carbonell, Phys. Rev. C **44**, 1281 (1991).
[9] J. S. Cohen and N. T. Padial, Phys. Rev. A **41**, 3460 (1990).
[10] S. Ahmad *et al.*, Phys. Lett. **157B**, 333 (1985); M. Ziegler *et al.*, Phys. Lett. B **206**, 151 (1988); C. W. E. Van Eijk *et al.*, Nucl. Phys. **A486**, 604 (1988); C. A. Baker *et al.*, *ibid.* **A483**, 631 (1988); R. Bacher *et al.*, Z. Phys. A **334**, 93 (1989).
[11] K. Heitlinger *et al.*, Z. Phys. A **342**, 359 (1992).
[12] R. A. Bryan and R. J. N. Phillips, Nucl. Phys. **B5**, 201 (1968).
[13] T. L. Trueman, Nucl. Phys. **26**, 57 (1961).
[14] A. M. Green and S. Wycech, Nucl. Phys. **A377**, 441 (1982).
[15] W. Schweiger, J. Haidenbauer, and W. Plessas, Phys. Rev. C **32**, 1261 (1985).
[16] J. Thaler, J. Phys. G **9**, 1009 (1983).
[17] W. B. Kaufmann and H. Pilkuhn, Phys. Rev. C **17**, 215 (1978); W. B. Kaufmann, Phys. Rev. C **19**, 440 (1979).
[18] M. A. Alberg, *et al.*, Phys. Rev. D **27**, 536 (1983).
[19] B. Moussallam, Z. Phys. A **325**, 1 (1986).
[20] J. Carbonell, G. Ihle, and J.-M. Richard, Z. Phys. A **334**, 329 (1989).
[21] C. B. Dover, J. M. Richard, and J. Carbonell, Ann. Phys. (N.Y.) **130**, 70 (1980).
[22] T. H. Burnett and S. R. Sharpe, Annu. Rev. Nucl. Part. Sci. **40**, 327 (1990); K. Peters, Nucl. Phys. **A558**, 93c (1993); G. Karl, *ibid.* **A558**, 113c (1993); C. B. Dover, *ibid.* **A558**, 721c (1993); C. Amsler, 27th International Conference on High Energy Physics, Glasgow, 1994 (unpublished).
[23] D. Alde *et al.*, Phys. Lett. B **205**, 397 (1988).
[24] Y. Yan and R. Tegen, Phys. Rev. C **54**, 1441 (1996).
[25] W. Buck, C. B. Dover, and J. M. Richard, Ann. Phys. (N.Y.) **121**, 47 (1979); C. B. Dover and J. M. Richard, *ibid.* **121**, 70 (1979); C. B. Dover, J. M. Richard, and M. C. Zabek, *ibid.* **130**, 70 (1980).
[26] J. M. Richard, M. Lacombe, and R. Vinh Mau, Phys. Lett. **64B**, 121 (1976); M. Lacombe, B. Loiseau, B. Moussallam, and R. Vinh Mau, Phys. Rev. C **29**, 1800 (1984).
[27] C. B. Dover, T. Gutsche, and A. Faessler, Phys. Rev. C **43**, 379 (1991).
[28] J. A. Niskanen and A. M. Green, Nucl. Phys. **A431**, 593 (1984).
[29] M. Maruyama and T. Ueda, Prog. Theor. Phys. **73**, 1211 (1985); **74**, 526 (1985).
[30] C. Amsler, Adv. Nucl. Phys. **18**, 183 (1988); C. Amsler and F. Myhrer, Annu. Rev. Nucl. Part. Sci. **41**, 219 (1991).
[31] Y. Yan, Ph.D. thesis, Universität Tübingen, 1994.
[32] E. Holoien, Phys. Rev. **104**, 1301 (1965).
[33] H. Schull and P.-O. Löwdin, J. Chem. Phys. **30**, 617 (1959).
[34] M. Rotenberg, Adv. At. Mol. Phys. **6**, 233 (1970).
[35] E. Truhlik, Nucl. Phys. **A296**, 134 (1978).
[36] B. Gyarmati, A. T. Kruppa, and J. Révai, Nucl. Phys. **A326**, 119 (1979); B. Gyarmati and A. T. Kruppa, *ibid.* **A378**, 407 (1982).
[37] B. Gyarmati, A. T. Kruppa, Z. Papp, and G. Wolf, Nucl. Phys. **A417**, 393 (1984).
[38] K. F. Pál, J. Phys. A **18**, 1665 (1985).
[39] J. Carbonell (private communication).
[40] G. Ihle, H. J. Pirner, and J.-M. Richard, Phys. Lett. B **183**, 15 (1987).
[41] Particle Data Group, L. Montanet *et al.*, Phys. Rev. D **50**, 1173 (1994).
[42] D. Bridges *et al.*, Phys. Rev. Lett. **56**, 211 (1986); **56**, 215 (1986); D. Bridges, I. Daftari, and T. E. Kalogeropoulos, *ibid.* **57**, 1534 (1986).
[43] C. Amsler *et al.*, Phys. Lett. B **291**, 347 (1992).
[44] V. V. Anisovich *et al.*, Phys. Lett. B **323**, 233 (1994); V. V. Anisovich *et al.*, Phys. Rev. D **50**, 1972 (1994).
[45] C. Amsler *et al.*, Phys. Lett. B **342**, 433 (1995).
[46] N. A. Tørnqvist, Phys. Rev. Lett. **67**, 556 (1991); K. Dooley, E. S. Swanson, and T. Barnes, Phys. Lett. B **275**, 478 (1992).
[47] M. Maruyama, S. Furui, and A. Faessler, Nucl. Phys. **A472**, 643 (1987); M. Maruyama, S. Furui, A. Faessler, and R. Vinh Mau, *ibid.* **A473**, 647 (1987); T. Gutsche, M. Maruyuma, and A. Faessler, *ibid.* **A503**, 737 (1989).
[48] C. B. Dover, T. Gutsche, M. Maruyama, and A. Faessler, Prog. Part. Nucl. Phys. **29**, 87 (1992).
[49] A. Adamo *et al.*, Nucl. Phys. **A558**, 13c (1993).
[50] D. Alde *et al.*, Phys. Lett. B **216**, 451 (1989); D. Alde *et al.*, *ibid.* **241**, 600 (1990).
[51] G. M. Beladidze *et al.*, Z. Phys. C **54**, 367 (1992).
[52] R. Machleidt, K. Holinde, and Ch. Elster, Phys. Rep. **149**, 1 (1987).
[53] W. N. Cottingham, M. Lacombe, B. Loiseau, J. M. Richard, and R. Vinh Mau, Phys. Rev. D **8**, 800 (1973).
[54] R. Thierauf, Ph.D. thesis, Universität Tübingen, 1994; R. Thierauf, T. Gutsche, Y. Yan, A. Muhm, and A. Faessler, Nucl. Phys. **A588**, 783 (1995).
[55] D. Gotta, Nucl. Phys. **A558**, 645c (1993).
[56] W. Weise, Nucl. Phys. **A558**, 219c (1993).
[57] F. Myhrer and R. Tegen, Phys. Lett. **126B**, 237 (1985).